The RNA m^{6}A reader YTHDF1 is required for acute myeloid leukemia progression

Yun-Guang Hong[1,#], Zhigang Yang[1,3,8,#], Yan Chen[1], Tian Liu[1], Yuyuan Zheng[2], Chun Zhou[2], Guo-Cai Wu[3], Yinhui Chen[4], Juan Xia[5], Ruiting Wen[3,8], Wenxin Liu[1,8], Yi Zhao[6], Jin Chen[7], Xiangwei Gao[1,*], and Zhanghui Chen[1,8,*].

[1] Zhanjiang Institute of Clinical Medicine, Zhanjiang Central Hospital, Guangdong Medical University, Zhanjiang, China.

[2] Zhejiang University School of Medicine, Hangzhou, China.

[3] Department of Hematology, Central People's Hospital of Zhanjiang, Zhanjiang, China.

[4] Department of Pediatrics, Affiliated Hospital of Guangdong Medical University, Zhanjiang, China.

[5] Department of Hematology, Affiliated Hospital of Guangdong Medical University, Zhanjiang, China.

[6] Bone Marrow Transplantation Center, the First Affiliated Hospital, Zhejiang University School of Medicine, Hangzhou, China.

[7] Department of Hematology, Yiwu Central Hospital, Yiwu, China.

[8] Zhanjiang Key Laboratory of Leukemia Pathogenesis and Targeted Therapy Research.

[#] These authors contributed equally.

[*] Correspondence: Zhanghui Chen, Email: zjcell@126.com, or Xiangwei Gao, Email: xiangweigao@zju.edu.cn.

SUPPLEMENTARY INFORMATION

Supplementary Methods

Supplementary Figures 1-8

Supplementary Methods

Flow cytometry analysis of BM and PB cells

For the detection of hematopoietic stem and progenitor cells, unfractionated BM cells were stained with Mouse Hematopoietic Lineage Antibody Cocktail (Cat#88-7772-72, eBioscience), anti-c-Kit (Cat#17-1171-81, eBioscience), anti-Sca-1 (Cat#11-5981-81, eBioscience), anti-CD150 (Cat#25-1502-82, eBioscience), anti-CD48 (Cat#12-0481-82, eBioscience), and anti-CD135 (Cat#46-1351-82, eBioscience). Gating for LSK ($Lin^-Sca\text{-}1^+c\text{-}Kit^+$), Prog ($Lin^-c\text{-}Kit^+$), MPP4 ($Lin^-Sca\text{-}1^+c\text{-}Kit^+CD48^+CD135^+$), MPP3 ($Lin^-Sca\text{-}1^+c\text{-}Kit^+CD135^-CD150^-CD48^+$), MPP2 ($Lin^-Sca\text{-}1^+c\text{-}Kit^+CD135^-CD150^+CD48^+$), LT-HSC ($Lin^-Sca\text{-}1^+c\text{-}Kit^+CD135^-CD150^+CD48^-$), and ST-HSC ($Lin^-Sca\text{-}1^+c\text{-}Kit^+CD135^-CD150^-CD48^-$) was applied. BM cells were stained with Mouse Hematopoietic Lineage Antibody Cocktail (Cat#88-7772-72, eBioscience), anti-c-Kit (Cat#17-1171-81, eBioscience), anti-Sca-1 (Cat#11-5981-81, eBioscience), anti-CD34 (Cat#56-0341-82, eBioscience), anti-CD16/32 (Cat#101333, BioLegend), anti-CD135 (Cat#46-1351-82, eBioscience), and anti-CD127 (Cat#25-1271-82, eBioscience). Gating for LMPP ($Lin^-Sca\text{-}1^+c\text{-}Kit^+CD135^+CD127^+$), CLP ($Lin^-Sca\text{-}1^{low}c\text{-}Kit^{low}CD135^+CD127^+$), GMP ($Lin^-Sca\text{-}1^-c\text{-}Kit^+CD34^+CD16/32^{hi}$), CMP ($Lin^-Sca\text{-}1^-c\text{-}Kit^+CD34^+CD16/32^{mid}$), and MEP ($Lin^-Sca\text{-}1^-c\text{-}Kit^+CD34^-CD16/32^{low}$) was applied. For competitive reconstruction assay, anti-CD45.2 (Cat#47-0454-82, eBioscience) was additionally added to the above antibody combination to detect the expression of CD45.2. PB cells were incubated with anti-CD3, anti-CD4, and anti-CD19 antibodies for the staining of T and B cells, while anti-CD11b and anti-Gr-1 antibodies were used for myeloid cells. To assess human AML burden, mice were sacrificed one month after transplantation. BM from mice were stained anti-human CD45 and CD117 antibodies.

Supplementary Figure 1

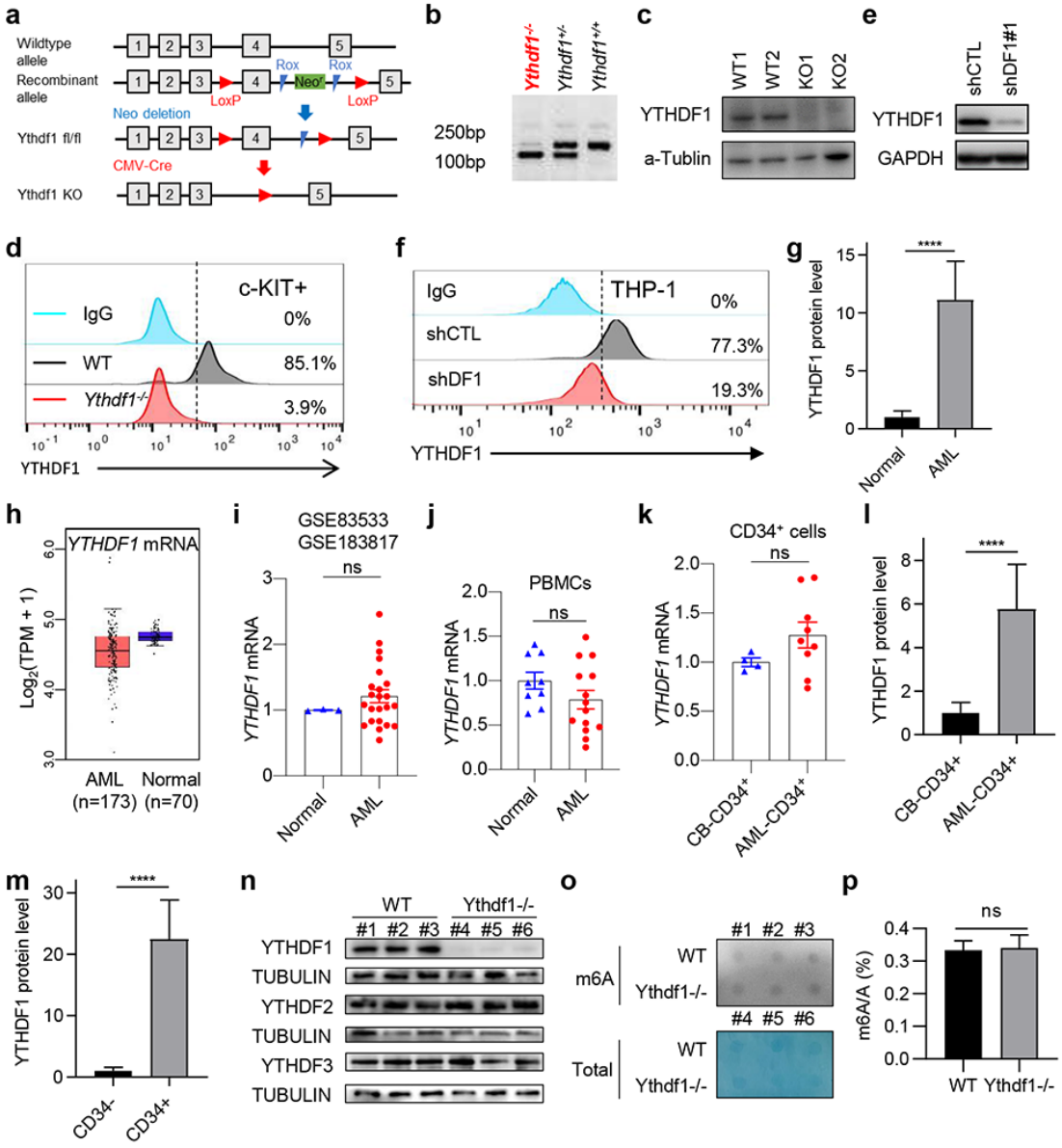

Supplementary Figure 1. The protein level of YTHDF1 is upregulated in AML.

(a) Strategy for generation of *Ythdf1* knockout mouse.

(b) The representative genotyping of WT or *Ythdf1*$^{-/-}$ mice.

(c) Immunoblot analysis of YTHDF1 expression in bone marrow cells from WT or *Ythdf1*$^{-/-}$ mice.

(d) FACS analysis of YTHDF1 expression in c-Kit^{+} cells from WT or *Ythdf1*$^{-/-}$ mice.

(e-f) Immunoblot (e) and FACS (f) analysis of YTHDF1 protein expression in control and YTHDF1 knockdown THP-1 cells.

(g) Quantification of immunoblot bands from Figure 1d. **** $p < 0.0001$, t-test.

(h) Box plot showing the relative expression of *YTHDF1* mRNA in normal and AML

samples from the TCGA database.
(i) Comparison of *YTHDF1* mRNA expression in healthy donors (n=3) vs primary AML patients (n=23) based on GEO datasets (GSE83533 and GSE183817). The quantitative data are represented as mean ± SEM. ns, not significant, t-test.
(j) Relative *YTHDF1* mRNA expression in PBMCs from Normal (n=9) and human AML patients (n=14). Data are represented as mean ± SEM. ns, not significant, t-test.
(k) Relative *YTHDF1* mRNA expression in normal cord blood-derived $CD34^+$ cells (n = 4) and AML patient-derived $CD34^+$ cells (n = 9). Data are represented as mean ± SEM. ns, not significant, t-test.
(l, m) Quantification of immunoblot bands from Figure 1e and 1f. **** $p < 0.0001$, t-test.
(n) Immunoblot analysis of YTHDF1-3 expression in bone marrow cells from WT or *Ythdf1*$^{-/-}$ mice.
(o) m^6A dot blot assays of bone marrow cells from WT or *Ythdf1*$^{-/-}$ mice.
(p) Quantification of m^6A level of bone marrow cells using EpiQuik m^6A RNA Methylation Quantification Kit. ns, not significant, t-test.

Supplementary Figure 2

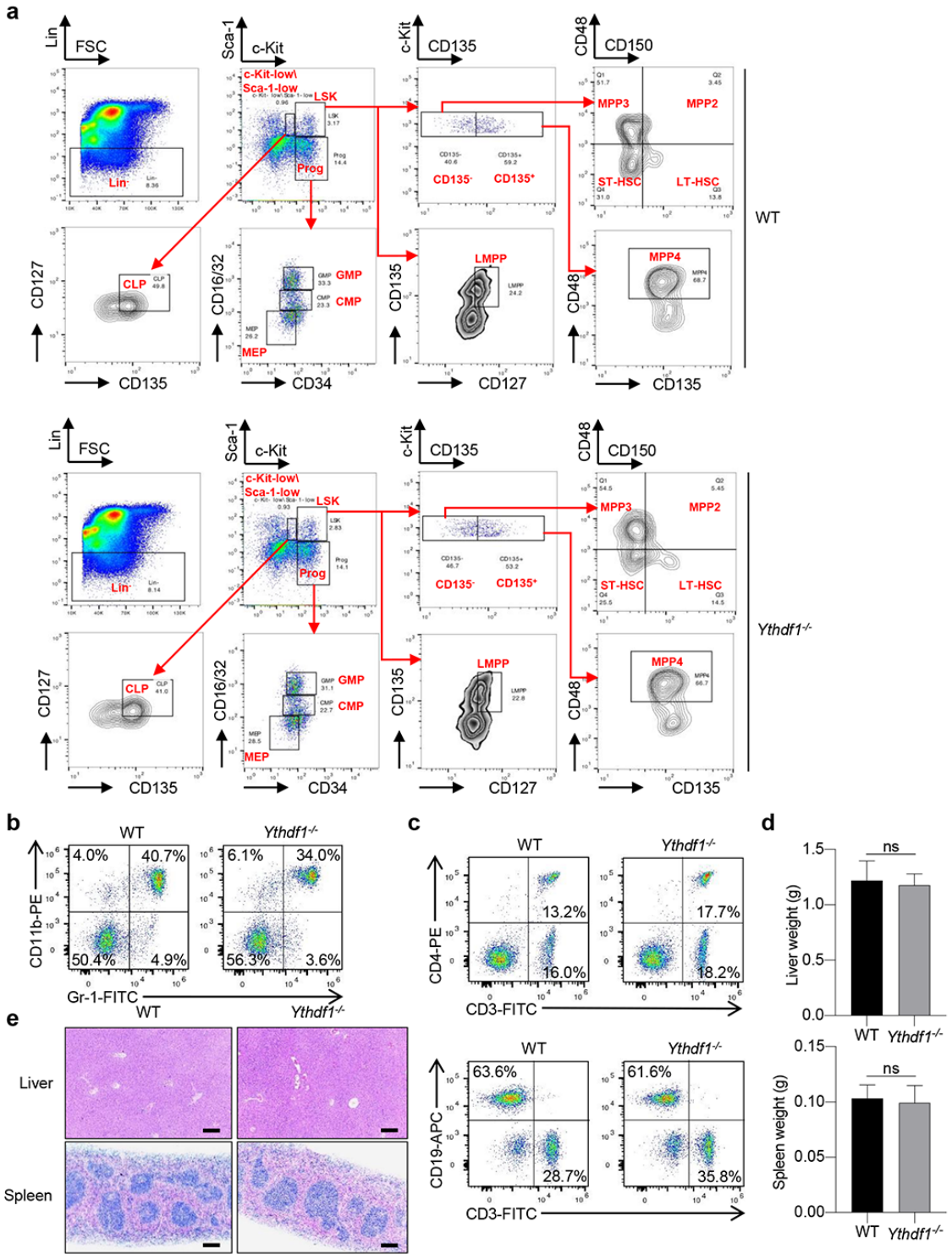

Supplementary Figure 2. Depletion of *Ythdf1* gene does not alter hematopoiesis in mice.

(a) Representative flow cytometry gating strategy for different stem/progenitor cell

populations in bone marrow from *Ythdf1*$^{-/-}$ mice and WT mice.
(b) Representative flow cytometry plot of peripheral blood (PB) terminal differentiated myeloid cell populations from *Ythdf1*$^{-/-}$ mice and WT mice.
(c) Representative flow cytometry plot of terminal differentiated B and T lymphocyte subpopulations from *Ythdf1*$^{-/-}$ mice and WT mice.
(d) The weight of liver and spleen from *Ythdf1*$^{-/-}$ mice and WT mice (n = 3, ns, not significant, t-test).
(e) Hematoxylin and eosin (H&E) staining of liver and spleen from *Ythdf1*$^{-/-}$ mice and WT mice. Scale bar, 100 μm.

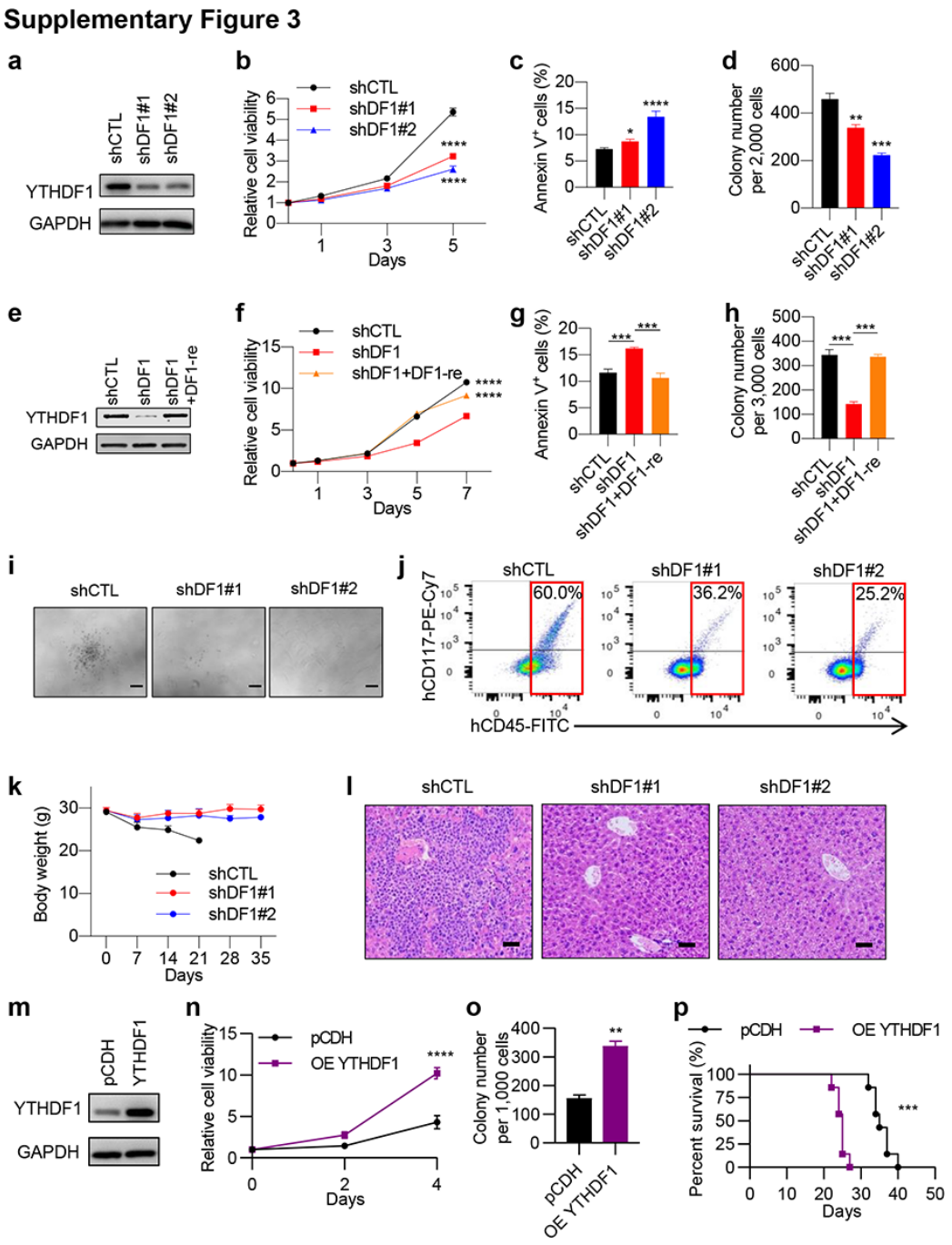

Supplementary Figure 3. YTHDF1 is essential for the progression of AML.

(a) Immunoblot analysis of YTHDF1 in control and YTHDF1 knockdown MV-4-11 cells. GAPDH was used as a loading control.

(b-d) Cell proliferation (b), annexin V (c), and colony-forming (d) analysis in control and YTHDF1 knockdown MV-4-11 cells. Data are represented as mean ± SEM (n = 3). * $p < 0.05$, ** $p < 0.01$, *** $p < 0.001$, **** $p < 0.0001$, t-test.

(e) Immunoblot analysis of YTHDF1 in control, YTHDF1 KD and rescue THP-1 cells.

GAPDH was used as a loading control.
(f-h) Cell proliferation (f), annexin V (g), and colony-forming (h) analysis of control, YTHDF1 KD and rescue THP-1 cells. Data are represented as mean ± SEM (n = 3). *** $p < 0.001$, **** $p < 0.0001$, t-test.
(i) Representative pictures of colonies from control and YTHDF1 knockdown AML patient-derived CD34+ cells as described in Figure 3j. Scale bar, 200 μm.
(j-l) NCG mice were injected with control or YTHDF1 knockdown AML patient-derived $CD34^+$ cells and analyzed as described in Figure 3l.
(j) Flow cytometry analysis of the percentage of human AML cells (human $CD45^+$ cells) in BM of recipient mice as described in Figure 3m.
(k) Body weight of recipient mice was demonstrated.
(l) Hematoxylin and eosin (H&E) staining of liver from recipient mice. Scale bar, 50 μm.
(m) Immunoblot analysis of YTHDF1 in control and YTHDF1 over-expression MV-4-11 cells. GAPDH was used as a loading control.
(n-o) Cell proliferation (n) and colony-forming (o) analysis of control and YTHDF1 over-expression MV-4-11 cells. The quantitative data are represented as mean ± SEM (n = 3). ** $p < 0.01$, **** $p < 0.0001$, t-test.
(p) Survival curve of NCG mice transplanted with control or YTHDF1 over-expression MV-4-11 cells (7 mice per group). *** $p < 0.001$, Mantel-Cox test.

Supplementary Figure 4

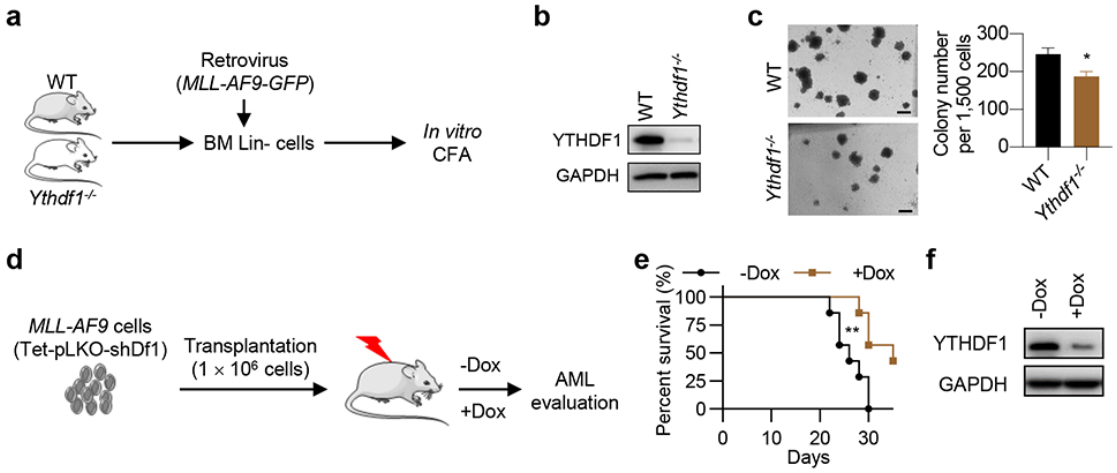

Supplementary Figure 4. YTHDF1 is required for murine AML development.
(a) Bone marrow (BM) lineage-negative (Lin-) cells collected from WT or Ythdf1-KO mice were transduced with *MLL-AF9-GFP* retrovirus and used for colony-forming assay (CFA).
(b) Immunoblot analysis of WT and Ythdf1-KO MLL-AF9 cells. GAPDH was used as a loading control.
(c) Colony-forming units of WT and Ythdf1-KO MLL-AF9 cells. The quantitative data are represented as mean ± SEM (n = 3). * $p < 0.05$, t-test. Scale bar, 200 μm.
(d) Schematic of *Ythdf1* inducible knockdown in MLL-AF9 model. *Ythdf1* shRNA1 was cloned into Dox-inducible vector Tet-pLKO (Tet-pLKO-shDf1). MLL-AF9 leukemia cells were infected with Tet-pLKO-shDf1 lentivirus and then transplanted into irradiated recipient mice. Mice were maintained for another two weeks for establishment of comparable engraftment. Doxycycline (Dox) chow containing 700 mg/kg doxycycline was given to induce *Ythdf1* knockdown.
(e) Survival curve of mice transplanted with Tet-pLKO-shDf1 leukemia cells with or without Dox treatment (7 mice per group). ** $p < 0.01$, Mantel-Cox test.
(f) Immunoblot analysis of GFP+ cells from mice with or without Dox treatment. GAPDH was used as a loading control.

Supplementary Figure 5

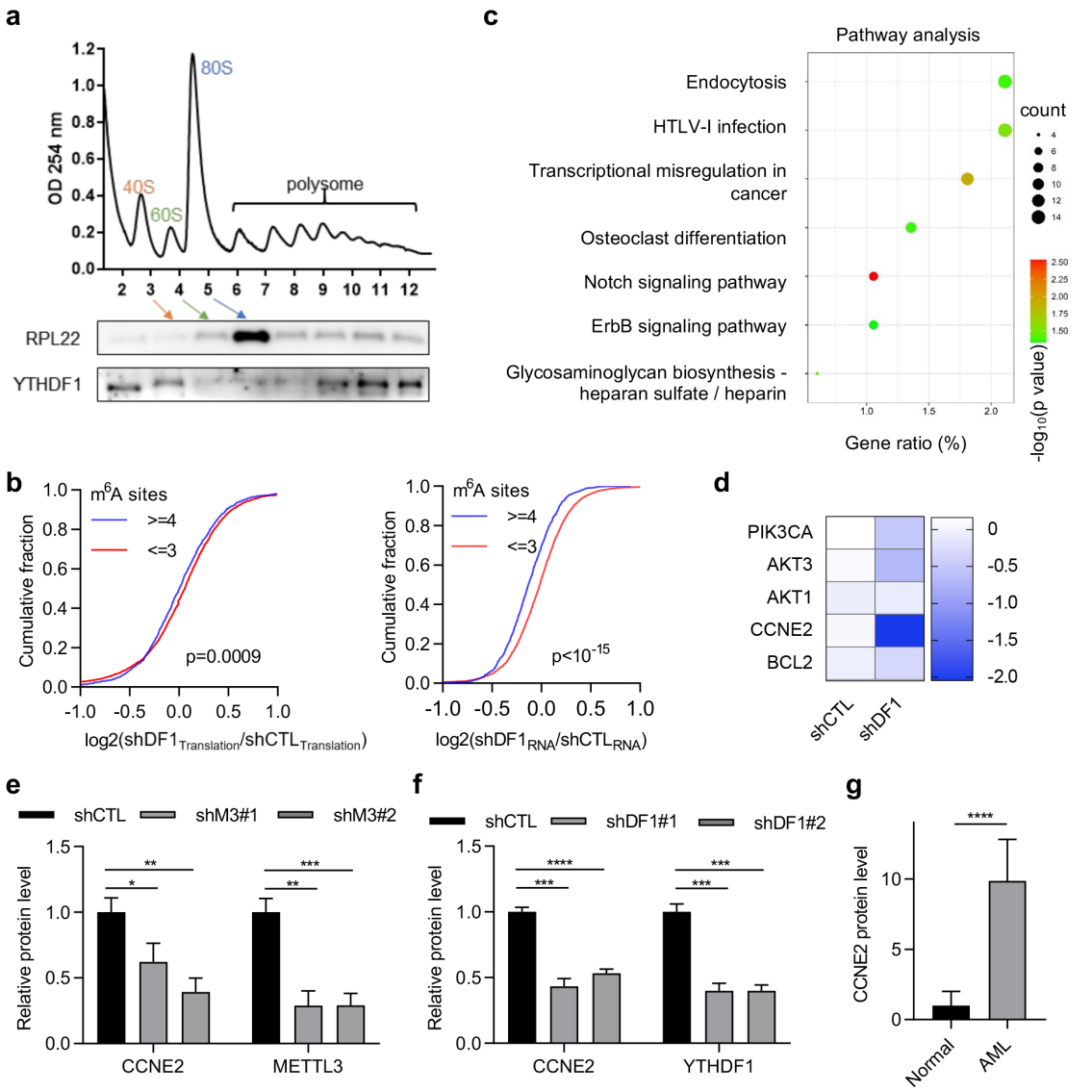

Supplementary Figure 5. Identification of YTHDF1-regulated transcripts.

(a) The distribution of YTHDF1 protein in the polysome fraction of THP-1 cells.

(b) Genes were divided into different groups based on the number of m^{6}A sites. Translation level and mRNA level for different group of genes were analyzed. Data are presented cumulative plots.

(c) KEGG enrichment analysis of YTHDF1 targets that are upregulated in YTHDF1-deficient cells.

(d) Heatmap showing the translational efficiency (TE) of PI3K-Akt signaling components in control and YTHDF1 knockdown cells. The values show the fold change of the indicated color of the heatmap.

(e,f,g) Quantification of immunoblot bands from Figure 5i,5j and 6b. * $p < 0.05$, ** $p < 0.01$, *** $p < 0.001$, **** $p < 0.0001$, t-test.

Supplementary Figure 6

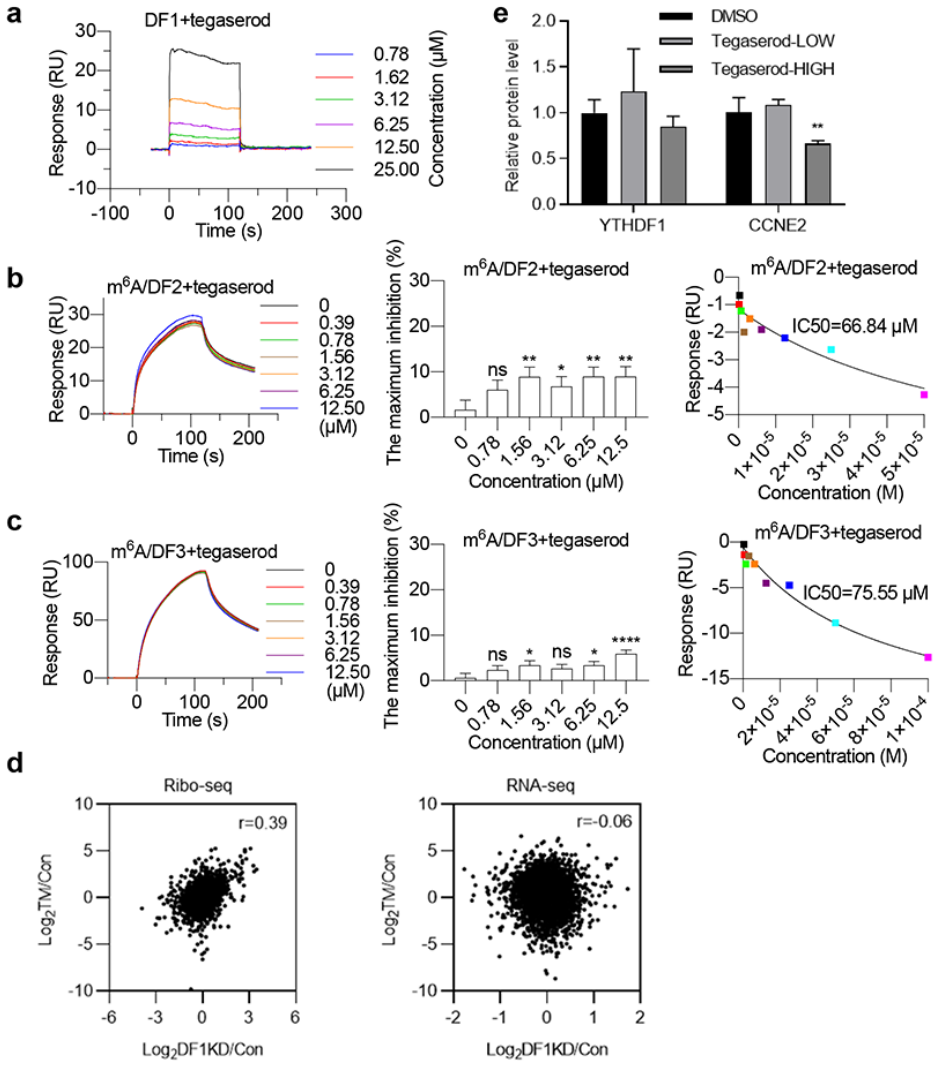

Supplementary Figure 6. The specificity of tegaserod on m^{6}A/YTHDF1 binding.

(a) Biacore assay of the binding between YTH domain of YTHDF1 and tegaserod.

(b) Effect of tegaserod on the interaction between m^{6}A-modified oligos and YTH domain of YTHDF2. * $p < 0.05$, ** $p < 0.01$, ns, not significant, t-test.

(c) Effect of tegaserod on the interaction between m^{6}A-modified oligos and YTH domain of YTHDF3. * $p < 0.05$, **** $p < 0.0001$, ns, not significant, t-test.

(d) Correlation analysis of RNA-seq data and Ribo-seq data in tegaserod-treated cells vs YTHDF1-knockdown cells.

(e) Quantification of immunoblot bands from Figure 7f. ** $p < 0.01$, t-test.

Supplementary Figure 7

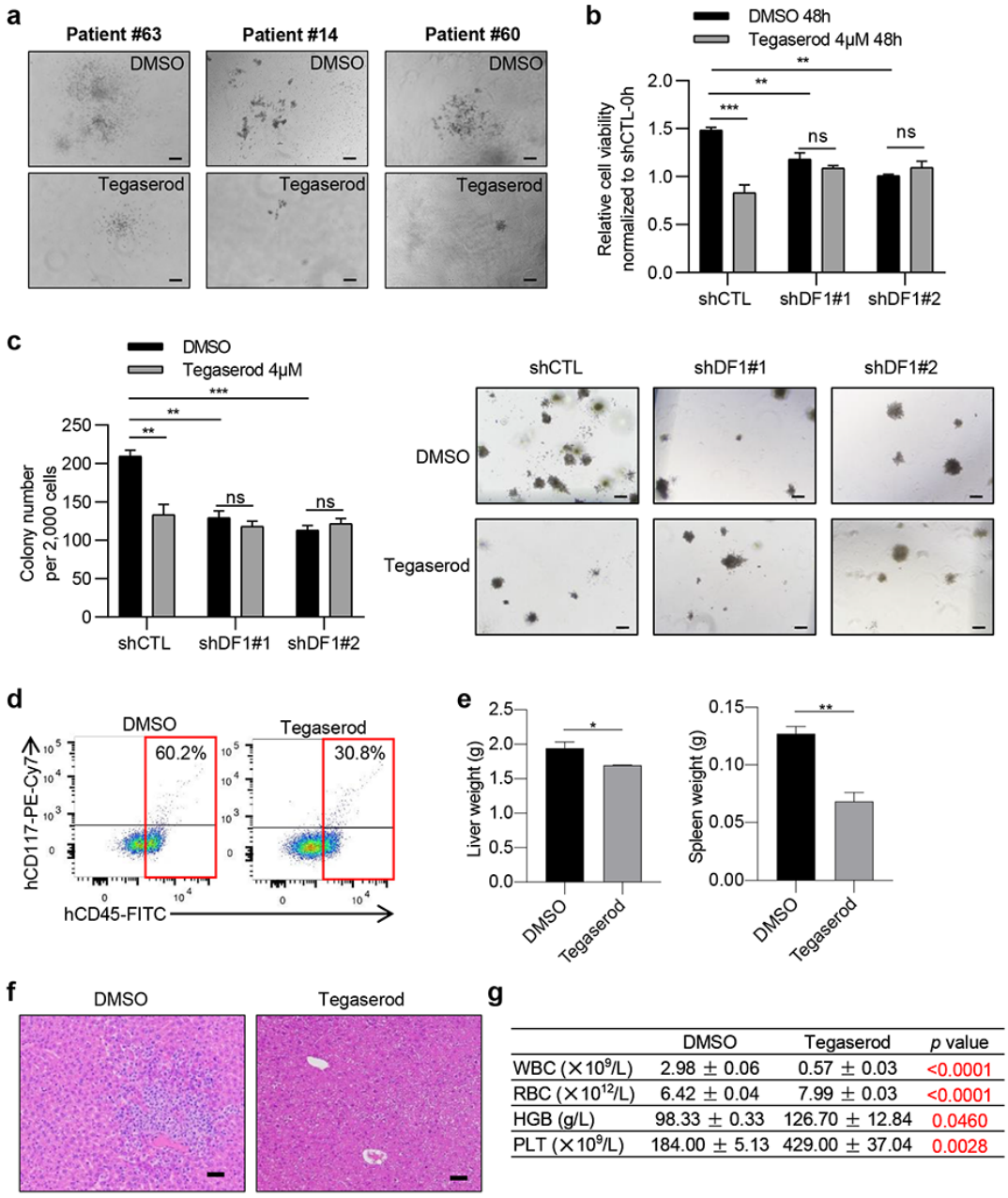

	DMSO	Tegaserod	*p* value
WBC ($\times 10^9$/L)	2.98 ± 0.06	0.57 ± 0.03	<0.0001
RBC ($\times 10^{12}$/L)	6.42 ± 0.04	7.99 ± 0.03	<0.0001
HGB (g/L)	98.33 ± 0.33	126.70 ± 12.84	0.0460
PLT ($\times 10^9$/L)	184.00 ± 5.13	429.00 ± 37.04	0.0028

Supplementary Figure 7. Tegaserod impedes AML progression and prolongs survival.

(a) Representative pictures of colonies from AML patient-derived $CD34^+$ cells treated with DMSO or tegaserod maleate as described in Figure 8e. Scale bar, 200 μm.

(b, c) Cell proliferation (b) and colony-forming (c) analysis of control and YTHDF1 KD THP1 cells with or without tegaserod treatment. Data are represented as mean ± SEM (n = 3). ** $p < 0.01$, *** $p < 0.001$, ns, not significant, t-test. Scale bar, 200 μm.

(d) Flow cytometry analysis of the percentage of human AML cells (human $CD45^+$) in

BM of mice treated with tegaserod maleate or DMSO as described in Figure 8h.
(e) The weight of liver and spleen from AML patient-derived $CD34^+$ cells-transplanted mice treated with DMSO or tegaserod maleate. Data are represented as mean ± SEM (n = 3). * $p < 0.05$, ** $p < 0.01$, t-test.
(f) H&E staining of liver from AML patient-derived $CD34^+$ cells-transplanted mice treated with DMSO or tegaserod maleate. Scale bar, 50 μm.
(g) PB counts from AML patient-derived $CD34^+$ cells-transplanted mice treated with DMSO or tegaserod maleate. Data are represented as mean ± SEM (n = 3, t-test).

Supplementary Figure 8

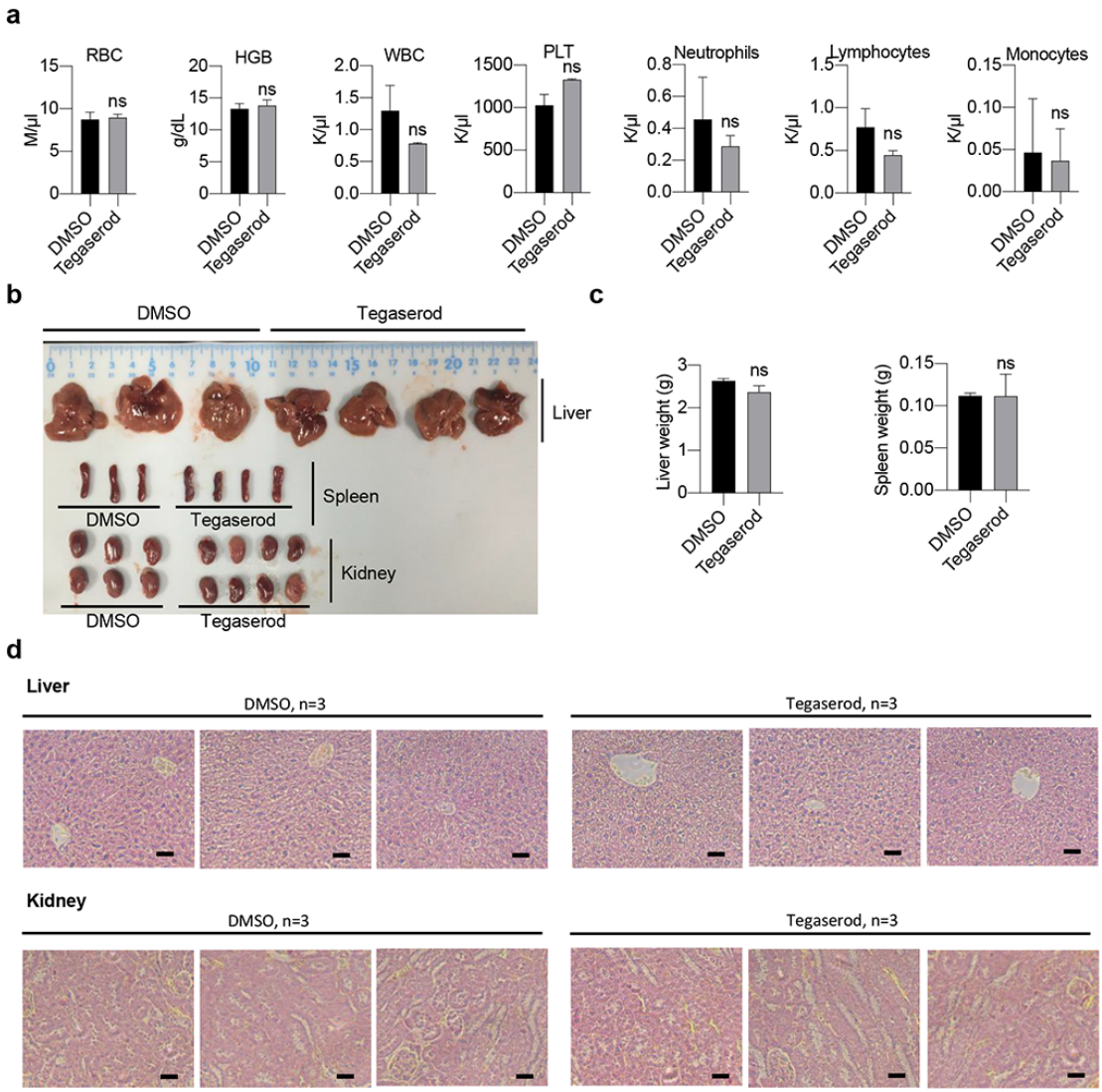

Supplementary Figure 8. The potential toxicities of evaluating tegaserod in *vivo*.
(a) Peripheral blood counts from mice treated with DMSO or tegaserod maleate. Data are represented as mean ± SEM (n = 3), ns, not significant, t-test.
(b-d) Effect of tegaserod maleate on liver, spleen and kidney from mice. Data are represented as mean ± SEM (n = 3), ns, not significant, t-test. Scale bar, 50 μm.